Precision measurements of fine and hyperfine structure in lithium I and II

W.A. van Wijngaarden

Abstract: Recent advances in modeling Li I and II in conjunction with improved experimental techniques have enabled precise tests of quantum electrodynamics. For Li^+, the hyperfine intervals of the 1s2s $^3S_1$ and 1s2p $^3P_{0,1,2}$ states are in excellent agreement with theory. A recent measurement of the 1s2p $^3P_{1,2}$ fine-structure interval also agrees well with the calculated value and resolves a discrepancy found by two prior experiments. For neutral lithium, discrepancies exist among the results of various experiments for the ^{6,7}Li D1 isotope shift and the 2P fine structure. However, all of the fine-structure measurements are several MHz larger than the theoretical value. Prospects for future experiments to improve the determination of the fine-structure constant and the relative ^{6,7}Li nuclear charge radii are discussed.

PACS Nos.: 32.10.Fn, 31.30.Gs, 42.62.Fi

Résumé : Des progrès récents dans la modélisation de Li I et II , couplés à une amélioration des techniques expérimentales, ont permis des test plus précis de QED. Pour Li^+, les séparations hyperfines des états 1s2s $^3S_1$ et 1s2p $^3P_{0,1,2}$ sont en excellent accord avec la théorie. Une mesure récente de la séparation de structure fine 1s2p $^3P_{1,2}$ agrée avec les valeurs calculées et résout un problème soulevé par deux expériences antérieures. Dans le lithium neutre, des divergences persistent parmi les résultats de diverses expériences sur le déplacement isotopique ^{6,7}Li D1 et sur la structure fine du 2P. Cependant, toutes les mesures de structure fine sont plusieurs MHz plus élevés que les valeurs théoriques. Nous discutons les possibilités pour de futures expériences d'améliorer la constante de structure fine et le rayon de charge des ^{6,7}Li.

[Traduit par la Rédaction]

1. Introduction

Hydrogenic atoms are the simplest atomic systems to model and, therefore, the best understood. However, it is difficult to apply precise laser spectroscopic techniques to study transitions from the ground state in such atoms that occur at wavelengths inaccessible to lasers. Most notably, the hydrogen $1s \rightarrow 2p$ transition at 121.5 nm lies in the vacuum ultraviolet part of the spectrum. In contrast, the two- and three-electron systems lithium II and I, have visible transitions that are readily excited using either continuous wave dye or diode lasers. The Li^+ 1s2s $^3S_1$ metastable state, which has a lifetime of 59 s [1], has a transition to the 1s2p $^3P_{0,1,2}$ state at a wavelength of 548 nm while the lithium D lines occur at 670 nm. Another advantage of studying Li^+ and neutral Li is that quantum electrodynamic (QED) effects that scale to lowest order as $Z^4\alpha^3$ times the Rydberg energy where Z is the nuclear charge and

Received 29 September 2004. Accepted 6 January 2005. Published on the NRC Research Press Web site at http://cjp.nrc.ca/ on 11 May 2005.

W.A. van Wijngaarden. Department of Physics, Petrie Bldg., York University, 4700 Keele St., Toronto, ON M3J 1P3, Canada (e-mail: wlaser@yorku.ca).

α is the fine-structure constant, are up to an order of magnitude larger than in hydrogen or helium.

Multielectron atoms are considerably more difficult to model as simple analytic solutions to the Schrödinger equation are not available. However, in the last decade major advances in many-body theory have been made [2] particularly by Drake and collaborators in developing the so-called Hylleraas variational technique [3]. The latter can determine highly accurate wave functions corresponding to the nonrelativistic portion of the Hamiltonian that can then be used to perturbatively evaluate higher order corrections due to relativistic, nuclear, and QED effects.

The combination of improved theory and precise measurements of isotope shifts has enabled the determination of relative nuclear charge radii [4]. In the case of ^{6,7}Li, this quantity has been determined with an order of magnitude smaller uncertainty than was found using electron scattering [5, 6]. Similar measurements are underway to study the radioactive isotopes ^{8,9,11}Li, which are predicted to have so-called halo neutrons [7].

A number of different experimental techniques have been applied to precisely study Li^+ and neutral Li. Unfortunately, significant discrepancies between the various experiments exist. In the case of the Li^+ 1s2p $^3P_{1,2}$ fine-structure interval, two experiments reported results differing by 11 MHz which is approximately 17 times the quoted one standard deviation measurement uncertainty [5, 8]. For neutral lithium, there have been problems calibrating Fabry–Perot interferometers necessitating the remeasurement of fine-structure and isotope shifts [9, 10].

The purpose of this paper is to compare the most precise experimental results with theoretical calculations and outline prospects for future improvements. The experimental techniques are discussed briefly as detailed descriptions of all methods including experiments yielding less accurate results are reviewed elsewhere [11]. The paper is organized as follows. First the experimental technique that uses a laser beam modulated by an electro-optic modulator to measure frequency intervals is described. Next, its application to study the Li^+ 1s2p $^3S_1 \rightarrow$ 1s2p $^3P_{0,1,2}$ transition and the neutral lithium D lines is discussed. The measurements are compared to theory and prospects for improved experiments are presented.

2. Frequency-interval determination using an electro-optically modulated laser beam

A common method to determine frequency intervals is to laser excite an atomic or ion beam [9, 10]. The laser frequency ν is scanned across the resonance while a photomultiplier detects fluorescence produced by the radiative decay of the excited species. The change in laser frequency is determined by passing part of the laser beam through an etalon whose free spectral range was previously determined at a national standards laboratory. Careful etalon calibration is critical. For example, a 1 m confocal etalon has a free spectral range of 75 MHz. Hence, the etalon free spectral range must be determined to better than 1 kHz to determine a 10 GHz frequency interval with an uncertainty of 0.1 MHz. Unfortunately, these experiments are unable to monitor any change in the etalon calibration due to fluctuations in temperature, pressure, vibrations, etc. Indeed, maintaining proper calibration even for etalons housed in a temperature-stabilized vacuum chamber, has proved problematic [9, 10].

An alternative method is illustrated in Fig. 1 that uses a frequency-modulated laser. The latter can be generated using either an electro- or acousto-optic modulator [11, 12]. Electro-optic modulators in general operate at higher frequencies than acousto-optic modulators and the various laser-frequency components are collinear rather than being spatially separated. The modulation frequency ν_{mod} is easily specified to one part per million by a frequency generator. For the experiments described here, electro-optic modulators operating at 6.8 and 9.2 GHz were used. The laser beam excites either an atomic or ion beam and fluorescence is detected as the laser frequency is scanned across the resonance. Each transition generates multiple peaks in the observed spectrum corresponding to excitation by the various laser-frequency components. The frequency axis can then be calibrated using the modulation frequency.

A key advantage of this technique is that each laser scan is independently calibrated. Furthermore, a

Fig. 1. Schematic diagram of apparatus required to determine frequency intervals using a laser that passes through an electro-optic modulator (EOM) to excite an ion or atomic beam. Fluorescence is observed by a photomultiplier tube (PMT) while a photodiode (PD) detects the transmission of the laser through an etalon as described in the text.

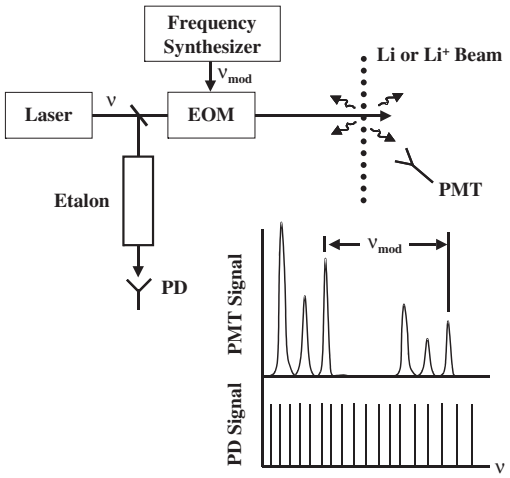

Fig. 2. Relevant energy levels of Li^+. The dominant decay rates are 2.27×10^7 s^{-1} for the 1s2p $^3P_{0,1,2} \rightarrow$ 1s2s $^3S_1$ transition and 1.79×10^4 s^{-1} for the 1s2p $^3P_2 \rightarrow (1s)^2$ $^1S_0$ transition. The other decay rates shown are doubly forbidden and, therefore, several orders of magnitude smaller.

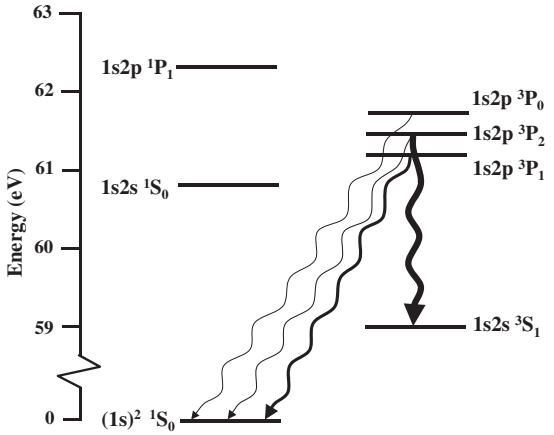

relatively large frequency interval such as 10 GHz can be determined by measuring a smaller interval of 800 MHz and adding the 9.2 GHz modulation frequency. Hence, a determination of a 10 GHz interval with an uncertainty of one part in 10^5 only requires measuring the 800 MHz interval with an uncertainty of one part in 8000. Moreover, this method is less sensitive to the effect of any nonlinearity of the laser frequency scan. Finally, only a single laser is required as compared to other techniques that determine intervals by measuring the frequency difference of two separate lasers that are each locked to a different energy level.

2.1. Li^+ 1s2s $^3S_1 \rightarrow$ 1s2p $^3P_{0,1,2}$ transition

Figure 2 illustrates the relevant Li^+ energies. Lithium ions are generated by colliding electrons accelerated by a few hundred volts with neutral lithium atoms. Typically 0.1% of the ions are generated in the metastable 1s2s $^3S_1$ state. This state can then be excited using a commercial ring dye laser

Fig. 3. Hyperfine Levels of 1s2s $^3S_1$ and 1s2p $^3P_{0,1,2}$ states of $^{6,7}Li^+$. The vertical energy axis is not drawn to scale. The hyperfine splittings for $^7Li^+$ are larger than $^6Li^+$. For example, the 1s2s $^3S_1$ splitting for the $^7Li^+$ 3/2→5/2 interval is 19.8 GHz whereas the corresponding $^6Li^+$ 1→2 interval is 6.0 GHz.

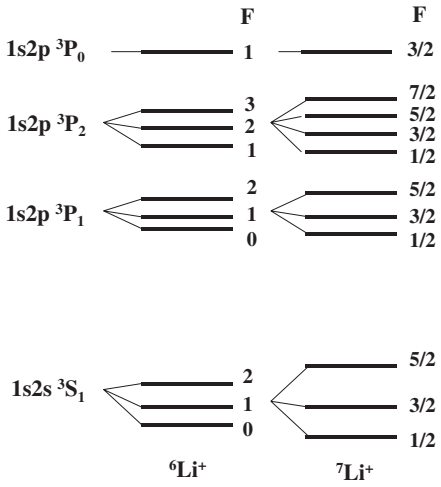

Fig. 4. Excitation of $^6Li^+$ 1s2s $^3S_1$ → 1s2p $^3P_2$ transition. The spectrum was obtained using (*a*) an unmodulated laser beam and (*b*) a laser beam that passed through an electro-optic modulator supplied with 1.7 W of power at a frequency of 9.200 000 GHz.

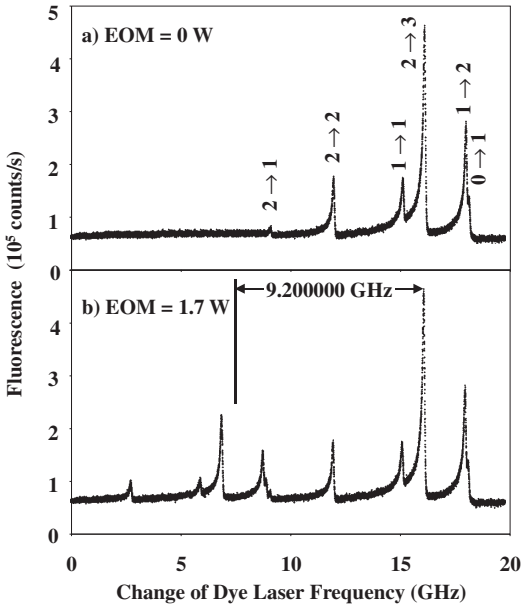

operating at 548 nm to examine transitions to the various hyperfine levels of the 1s2p $^3P_{0,1,2}$ state shown in Fig. 3 [13].

A sample spectrum is shown in Fig. 4. This was generated using anticollinear laser and ion beams. Fluorescence was recorded using a photomultiplier connected to a photon-counting apparatus as the laser frequency was scanned across the resonance. Data in Figs. 4*a* and 4*b* were taken using powers of 0 and 1.7 W, respectively, supplied to the electro-optic modulator. Two peaks corresponding to each transition are evident in Fig. 4*b*.

Fig. 5. Calibration of frequency scan. This was done using the two peaks separated by 9.200 000 GHz labeled in the preceding figure. One peak (black dots) was shifted and multiplied by an amplification factor as discussed in the text.

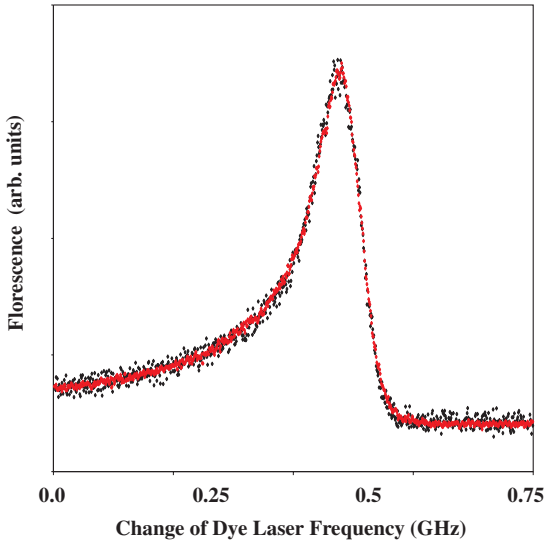

Table 1. $^{6}Li^{+}$ hyperfine intervals. The experimental results are obtained from ref. 13 unless otherwise indicated while the theoretical values are taken from ref. 5.

Level	Interval (F $\rightarrow$F′)	Experiment (MHz)	Theory (MHz)
1s2s $^{3}S_{1}$	2 $\rightarrow$ 1	6003.600 $\pm$ 0.050 [14]	6003.614 $\pm$ 0.024
		6003.66 $\pm$ 0.51	
	1 $\rightarrow$ 0	3001.780 $\pm$ 0.050 [14]	3001.765 $\pm$ 0.038
		3001.83 $\pm$ 0.47	
1s2p $^{3}P_{1}$	2 $\rightarrow$ 1	2888.98 $\pm$ 0.59	2888.327 $\pm$ 0.029
	1$\rightarrow$ 0	1316.06 $\pm$ 0.59	1317.649 $\pm$ 0.046
1s2p $^{3}P_{2}$	3$\rightarrow$ 2	4127.16 $\pm$ 0.76	4127.882 $\pm$ 0.043
	2 $\rightarrow$ 1	2857.00 $\pm$ 0.72	2858.002 $\pm$ 0.060

The conversion of the laser scan in units of time to frequency is accomplished by determining the time separating two peaks generated by the same ion transition but a different laser-frequency component. For example, Fig. 5 shows the overlap of the two peaks separated in Fig. 4*b* by the 9.200 000 GHz modulation frequency when one peak is shifted and multiplied by an amplification factor. Note the two peaks have the same asymmetric shape, which is due to the distribution of ion velocities.

The results for the $^{6}Li^{+}$ hyperfine intervals are shown in Table 1. For the 1s2s $^{3}S_{1}$ state, the experimental results agree closely with those obtained by a microwave experiment [14]. Experimental data for both the $^{6,7}Li^{+}$ 1s2s $^{3}S_{1}$ and 1s2p $^{3}P_{1,2}$ states agree very well with the Hylleraaas variational calculations. Indeed, 12 (13) of the measured hyperfine intervals are within 2σ (3σ) of the theoretical values where σ is the quoted uncertainty.

Table 2 lists the results for the Li^{+} 1s2p $^{3}P_{1-2}$ fine-structure interval. The result of Clarke et al. [13] agrees with the work of Riis et al. [5] who precisely measured absolute laser frequencies for transitions to the various fine-structure levels using a fast-ion beam. The laser heterodyne experiment by Rong et al. [8] used two frequency-locked dye lasers. One laser was locked using the fluorescence signal generated by laser excitation of the Li^{+} beam while the other was locked to an iodine transition using saturation

Table 2. Li^+ 1s2p $^3P_{1-2}$ fine-structure interval.

Result (MHz)	Technique
62 667.4 ± 2.0	Laser heterodyne [8]
62 678.41 ± 0.65	Fast beam [5]
62 679.46 ± 0.98	Electro-optically modulated laser beam [13]
62 679.4 ± 0.5	Hylleraas variational [5]

absorption spectroscopy. Parts of the two laser beams were focused onto a fast photodiode that was connected to a frequency counter that measured the frequency difference. The results of our experiment and the work of Riis et al. [5] agree very well with the theoretical result found using Hylleraas variational theory in contrast to that of Rong et al. [8]

2.2. Future prospects

The principal factor limiting our experimental accuracy is the asymmetry of the observed fluorescence peaks that affects the determination of line center. If the ions were cooled as is discussed in the next section, the determination of line center would be limited by the natural linewidth of the 1s2s $^3S_1 \rightarrow$ 1s2p ^3P transition. This FWHM linewidth, estimated using the 44 ns radiative lifetime of the 1s2p ^3P state, is only 3.7 MHz.

It is worthwhile noting that the 1s2p $^3P_{0-1}$ and $^3P_{1-2}$ fine-structure intervals of 155.7 and 62.5 GHz, respectively, are considerably larger than the corresponding intervals in He that have been used to determine the fine-structure constant α [15]. Hence, an experiment that determined the line center of transitions to the Li^+ 1s2p $^3P_{0-1}$ fine-structure levels to 0.1% of the natural transition linewidth, as has been done by several experiments in He [15, 16], could determine the fine-structure constant to one part in 4×10^8. This would be competitive with the most precise value of α, which is presently obtained from the measurement of the electron's anomalous magnetic moment (g-2) [17]. It would also test the Hylleraas theory for two systems He and Li^+ and, hopefully, resolve the discrepancy in the determinations of α obtained by the various experiments [17, 18].

2.2.1. Ion trap

The ultimate reduction in ion velocity is achieved by storing an ion in a Paul trap and applying laser-cooling techniques [19]. Indeed, the Li^+ 1s2s $^3S_1$ state was loaded into a Paul trap by an experiment over two decades ago [1]. The ions were, however, not laser cooled, as these techniques had not then been fully developed. Laser cooling to temperatures of milliKelvins could be done by tuning the laser slightly below the $^6Li^+$ 1s2s $^3S_1$ (F=2) $\rightarrow$ 1s2p $^3P_2$ (F=3) transition frequency. A typical cooling time found by estimating the time required to absorb and reradiate 10^4 photons is less than 0.5 ms.

The 1s2p $^3P_2$ state dominantly decays to the 1s2s $^3S_1$ state. It also, however, has a decay channel to the $(1s)^2$ $^1S_0$ ground state as illustrated in Fig. 2 but this is a $^3P_2 \rightarrow {}^1S_0$ transition that is doubly forbidden as compared with the $^3P_{0,1} \rightarrow {}^1S_0$ transitions [20]. Hence, the trap lifetime would be limited by the nearly 1 min lifetime of the 1s2s $^3S_1$ state assuming that a suitably high vacuum was maintained to minimize loss of trapped ions due to collisions with background gas atoms.

The trapped ions would be studied using a probe laser tuned to excite transitions between the various fine-structure levels of the 1s2s $^3S_1$ and 1s2p ^3P states. A probe laser beam could be generated by frequency shifting part of the cooling laser beam. An acousto-optic modulator can conveniently generate shifts up to a few GHz, which correspond to the hyperfine-structure intervals of the $^6Li^+$ 1s2s $^3S_1$ state. $^7Li^+$ would be more difficult to study using a single laser as the hyperfine-structure intervals of the 1s2s $^3S_1$ state are much larger than for $^6Li^+$.

Fig. 6. Relevant neutral lithium energy levels

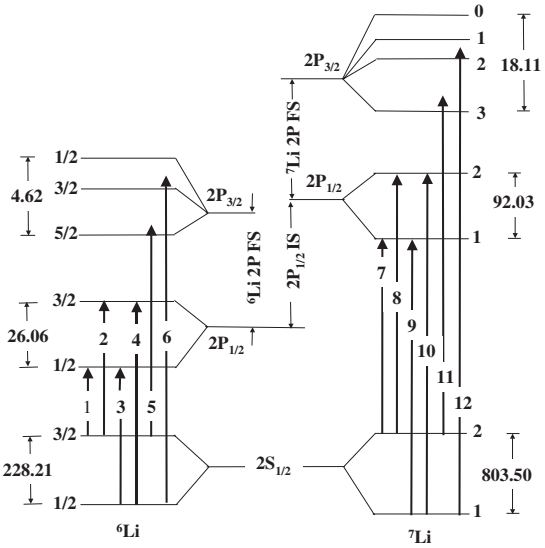

2.2.2. Optical double-resonance experiment

An optical double-resonance experiment [21] would first use a laser to excite the 1s2s ^{3}S state to one of the fine-structure levels of the 1s2p ^{3}P state. A microwave frequency would be applied next causing a transition to another fine-structure level. The detection of the transition among the 1s2p ^{3}P fine-structure intervals is difficult as typically only a small fraction of the atoms undergo this transition. It is, therefore, critical to design the experiment to enhance the detection of the microwave transition.

We consider the case of $^6Li^+$ for the reasons mentioned in the preceding section and show how the 1s2p $^3P_{1-2}$ fine-structure interval can be determined. The experiment would be done using lasers to perturb an ion beam as it passes through three successive regions. First, a laser beam would deplete the 1s2s $^3S_1$ (F=0) hyperfine level by exciting it to the 1s2p $^3P_1$ (F=1) level, which, in turn, can decay to any of the three hyperfine levels of the 1s2s $^3S_1$ state. The ions would then travel to a second region where a second laser beam would excite the 1s2s $^3S_1$ (F=1) $\rightarrow$ 1s2p $^3P_1$ (F=2) transition. This second laser beam would be generated by frequency shifting part of the first laser beam using an acousto-optic modulator. Microwaves exiting a wave guide would then induce the 1s2p $^3P_1$ (F=2) $\rightarrow$ 1s2p $^3P_2$ (F=1) transition. Ions in the 1s2p $^3P_2$ (F=1) level unlike ions in the 1s2p $^3P_1$ (F=2) level can radiatively decay to the 1s2s $^3S_1$ (F=0) level that was previously depopulated. The final stage of the experiment probes whether the microwave transition occurred by using part of the first laser beam to excite the 1s2s $^3S_1$ (F=0) $\rightarrow$ 1s2p $^3P_1$ (F=1) transition and detecting the fluorescence produced by the subsequent radiative decay.

This experiment requires generation of several watts of microwaves at frequencies corresponding to the fine-structure intervals. Present technology can quadruple a 0–20 GHz signal produced by a frequency synthesizer permitting the determination of the 1s2p $^3P_{1-2}$ fine-structure interval and associated hyperfine intervals. A future determination of the 1s2p $^3P_{0-1}$ fine-structure interval is contingent on the development of a precise microwave source operating near 150 GHz.

2.3. Lithium D lines

Figure 6 illustrates the hyperfine and fine-structure levels that generate the ^{6,7}Li D lines. Walls et al. [22] utilized an electro-optically modulated laser beam to scan an atomic beam to study these transitions using a diode laser modulated using an electro-optic modulator operating at either 6.8 or 9.2 GHz. The modulation frequency was chosen to avoid overlap of the various peaks in the spectrum. Fluorescence

Fig. 7. Fluorescence recorded as the diode laser was scanned across (*a*) the ^{6}Li D lines and (*b*) primarily the ^{7}Li D lines. The change in background occurring after 8 s in Fig. 7*a* and after 3.5 s in Fig. 7*b* resulted from insertion of a neutral density filter to attenuate the laser beam and thereby avoid saturation of the photomultiplier detected fluorescence signal.

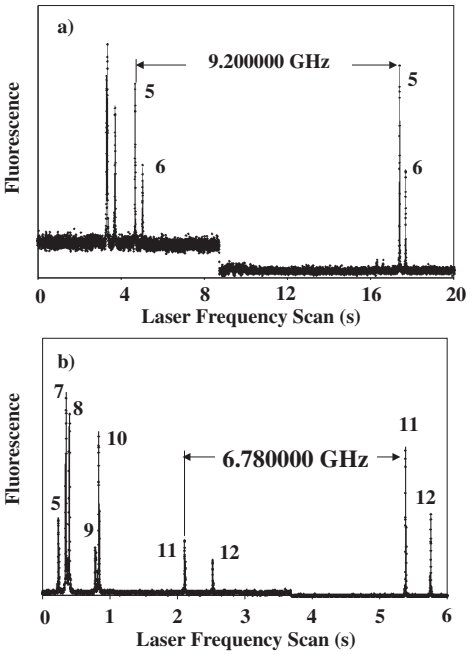

Fig. 8. Close up of fluorescence and fitted spectrum for laser frequency scans across the (*a*) ^{6}Li D transitions and (*b*) transition 11 as defined in Fig. 6.

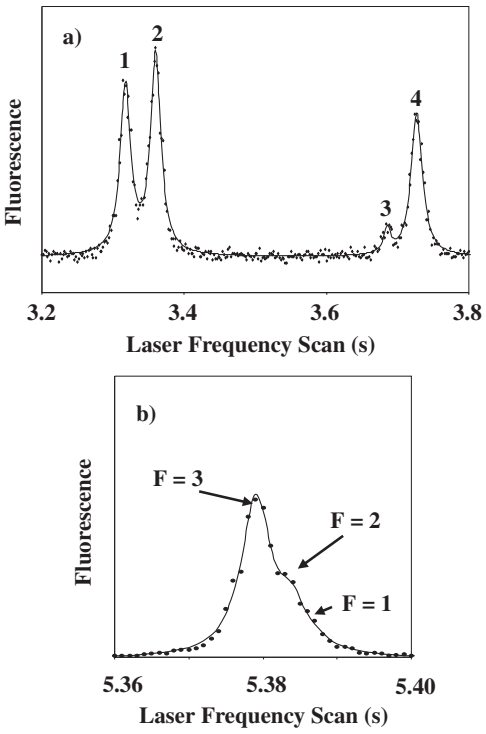

was recorded as the laser was scanned across the resonance. The frequency separating transitions 1 to 12 defined in Fig. 6 is over 20 GHz and exceeded the maximum laser scan range. The spectrum was, therefore, divided into two scans as shown in Fig. 7.

The fluorescence peaks were fitted to Lorentzian functions to determine the locations of the peak centers. Figure 8*a* shows the fitted spectrum for the transitions 1 to 4 corresponding to the ^{6}Li D1 lines that appear in Fig. 7*a* as the first two peaks. The determination of line centers is complicated when the excited-state hyperfine levels are not resolved. Figure 8 shows the fluorescence signal arising from transition 11. The fitted peak is a convolution of three Lorentzian functions because the hyperfine splittings of the ^{7}Li $2P_{3/2}$ state are comparable to the 5.8 MHz natural transition linewidth. Optical pumping effects must be taken into account when determining transitions to the various hyperfine levels.

The experimental technique was tested by measuring the ground-state hyperfine interval and comparing it to the very precise value determined using an atomic-beam magnetic-resonance method [23]. Table 3 shows that the results of Walls et al. [22] for both ^{6,7}Li are in excellent agreement with the known value. Similarly, the results for the magnetic dipole hyperfine constant for the ^{6,7}Li $2P_{1/2}$ states are in reasonable agreement with the very best results determined by an optical double resonance experiment [24]. Three theoretical groups have estimated the magnetic dipole constant for the ^{7}Li $2P_{1/2}$ state. The result obtained using the full core plus correlation method is less than either experimentally determined result [25] while two multiconfiguration Hartree–Fock theory estimates lie between the measured values [26, 27].

Table 3. Determination of hyperfine (HFS) and fine-structure (FS) intervals and isotope shift (IS) in ^{6,7}Li. MR = magnetic resonance, LC = level crossing, ODR = optical double resonance, LAB = laser atomic beam, FCPC = full core plus correlation, MCHF = multiconfiguration Hartree–Fock, HV = Hylleraas variational.

	Experiment		Theory	
Quantity	Result (MHz)	Technique	Result (MHz)	Technique
^{6}Li $2S_{1/2}$ HFS	228.205259	MR [23]		
	228.164 ± 0.064	LABEO [22]		
^{7}Li $2S_{1/2}$ HFS	803.5040866	MR [23]		
	803.534 ± 0.077	LABEO [22]		
^{6}Li a($2P_{1/2}$)	17.375 ± 0.018	ODR[24]		
	17.386 ± 0.031	LABEO [22]		
^{7}Li a($2P_{1/2}$)	45.914 ± 0.025	ODR [24]	45.793	FCPC [25]
	46.010 ± 0.025	LABEO [22]	45.984 ± 0.007	MCHF [26]
			45.945	MCHF [27]
D1 IS	10 533.13 ± 0.15	LAB [10]	10 534.13 ± 0.07 ± 0.61	HV [28]
	10 534.26 ± 0.13	LABEO [22]		
	10 533.16 ± 0.07	LAB [29]		
^{6}Li 2P FS	10 052.76 ± 0.22	LC [30]	10 050.85 ±.0.02 ± 3	HV [28]
	10 051.62 ± 0.20	LAB [10]		
	10 053.04 ± 0.09	LABEO [22]		
^{7}Li 2P FS	10 053.24 ± 0.22	LC [30]	10 051.24 ± 0.02 ± 3	HV [28]
	10 053.18 ± 0.06	ODR [31]		
	10 053.4 ± 0.2	LAB [10]		
	10 052.37 ± 0.11	LABEO [22]		

Table 3 also compares the experimental determinations of the ^{6,7}Li D1 isotope shift and the 2P fine-structure intervals with the results calculated using the Hylleraas variational theory [28]. The theoretical estimates list two uncertainties. The first number represents computational error while the second is due to the effect of higher order terms and the uncertainty in the relative ^{6,7}Li nuclear charge radius. The isotope shift measurement of Walls et al. [22] is in good agreement with theory in contrast to the result of two laser atomic beam measurements that rely on calibration of an interferometer [10, 29]. The isotope shift can be used to estimate the relative difference of the square of the nuclear radii for ^{6,7}Li. The measurement of Walls et al. [22] yields a value of 0.84 ± 0.08 fm^2 in agreement with the result of 0.73 ± 0.05 found by Riis et al. [5] who studied isotope shifts of the $1s2s\ ^3S_1 \rightarrow 1s2p\ ^3P_{0,1,2}$ transitions, and 0.79 ± 0.25 fm^2 obtained using electron scattering [6].

The various measurements of the 2P fine structure are not entirely consistent with each other but all experimental values are at least 1 MHz larger than the theoretical estimates. This is not entirely surprising as only terms in the Hamiltonian of order α^3 times the Rydberg energy were considered. For the case of helium, analogous terms of order α^4 contribute several MHz to the fine-structure splitting. It will be interesting to compare improved future experimental and theoretical results.

2.4. Future prospects

The accuracy of the determination of the 2P fine structure in the work of Walls et al. [5] is limited by the determination of the line center. This can be difficult when an observed fluorescence peak results from transitions to various unresolved hyperfine levels as is illustrated in Fig. 8*b*. A solution is to apply a magnetic field to Zeeman shift the levels to resolve transitions to the various hyperfine levels. The fine-structure splitting is then determined by taking data as a function of the magnetic field strength and extrapolating to zero magnetic field [32]. This obviously requires a carefully calibrated magnetic field

along with suitable cancellation of the Earth's field.

A second factor limiting the experimental accuracy is the laser scan nonlinearity. Instead, one could use two separate lasers each intersecting the atomic beam in different locations and exciting a different transition. Each laser would be frequency locked by maximizing the fluorescence signal. Part of each laser beam would be focused onto a fast photodiode connected to a frequency counter to measure the beat frequency. For the lithium 2P fine structure or ^{6,7}Li isotope shift, the beat frequency would be over 10 GHz. This frequency could be substantially reduced if one laser was frequency modulated. For example, a 9.2 GHz electro-optic modulator would reduce the beat frequency to less than 1 GHz which is readily measured.

The determination of a frequency interval by beating two frequency-locked lasers requires that each laser be locked to the transition center. A careful examination of the lineshape to understand possible asymmetries is critical. In practice, the experiment would be done by having the laser beams intersect the atomic beam orthogonally to eliminate first-order Doppler shifts. A misalignment of a few microradians for a 1 GHz Doppler-broadened line would shift an observed resonance by several kHz. Such a shift can be eliminated by passing each laser beam through a Fabry–Perot interferometer such that the laser beam is reflected back and forth many times through the atomic beam. This technique, which was recently used in helium, should be able to determine frequency intervals with a resolution of at least 10 kHz [16].

3. Conclusions

Considerable experimental and theoretical progress has been made especially in the case of Li^+. The experimental discrepancies have been resolved and all of the measured hyperfine and fine-structure intervals are in excellent agreement with the Hylleraas variational results. In the case of neutral lithium, inconsistencies between the results obtained by various experiments remain. Theory for neutral lithium, a three electron system, is also not as advanced as for Li^+. It is desirable to improve both theory and experiment to yield the 2P fine structure and D1 isotope shift to an uncertainty of less than 10 kHz. This will test QED in neutral lithium and reliably determine the relative ^{6,7}Li nuclear charge radius. Understanding the nuclear size is essential to allow future precision measurements of the Li^+ 1s2p ^{3}P fine-structure intervals to improve the determination of the fine-structure constant. Hence, interest in Li I and Li II will continue given the anticipated progress in both experiment and theory.

Acknowledgements

The author gratefully acknowledges the Canadian Natural Science and Engineering Research Council for financial support.

References

1. T. Knight and M. Prior. Phys. Rev. A, **21**, 179 (1980).
2. I. Lindgren, S. Salomonson, and B. Asen. Phys. Rep. **389**, 161 (2004).
3. Z.-C. Yan and G.W.F. Drake. Phys. Rev. Lett. **79**, 1646 (1997).
4. G.W.F. Drake, W. Nörtershäuser, and Z.-C. Yan. Can. J. Phys. **82**, 835 (2004).
5. E. Riis, H.G. Berry, O. Poulsen, S.A. Lee, and S.Y. Tang. Phys. Rev. A, **49**, 207 (1994).
6. C. de Jager, H. de Vries, and C. de Vries. At. Nucl. Data Tables, **14**, 479 (1974).
7. W. Nortershauser, A. Dax, G. Ewald et al. Nucl. Inst. B, **204**, 644 (2003).
8. H. Rong, S. Grafstrom, J. Kowalski, G. zu Putlitz, W. Jastrzekbski, and R. Neumann. Z. Phys. D, **25**, 337 (1993).
9. L. Windholz, H. Jager, M. Musso, and G. Zerza. Z. Phys. D, **16**, 41 (1990).
10. W. Scherf, O. Khait, H. Jager, and L. Windholz. Z. Phys. D, **36**, 31 (1996).
11. J. Clarke and W.A. van Wijngaarden. Recent Res. Develop. Phys. **3**, 347 (2002); W.A. van Wijngaarden. Proc. Int. Conf. At. Phys. **16**, 305 (1999).

12. W.A. van Wijngaarden. Adv. At. Mol. Opt. Phys. **36**, 141 (1996).
13. J. Clarke and W.A. van Wijngaarden. Phys. Rev. A, **67**, 012506 (2003).
14. J. Kowalski, R. Neumann, S. Noehte, K. Scheffzek, H. Suhr, and G. zu Putlitz. Hyp. Int. **15**, 159 (1983).
15. M. George, L. Lombardi, and E. Hessels. Phys. Rev. Lett. **87**, 173002 (2001).
16. P. Pastor, G. Giusfredi, P. De Natale, G. Hagel, C. de Mauro, and M. Inguscio. Phys. Rev. Lett. **92**, 023001 (2004).
17. P.J. Mohr and B.N. Taylor. J. Chem. Phys. Ref. Data, **28**, 1713 (1999); Rev. Mod. Phys. **72**, 351 (2000).
18. G.W.F. Drake. Can. J. Phys. **80**, 1195 (2002).
19. A.A. Madej and K.J. Siemsen. Opt. Lett. **21**, 824 (1996).
20. G.W.F. Drake. Phys. Rev. A, **19**, 1387 (1979).
21. A. Corney. Atomic and laser spectroscopy. Clarendon Press, Oxford. 1977.
22. J. Walls, R. Ashby, J.J. Clarke, B. Lu, and W.A. van Wijngaarden. Eur. Phys. J. D, **22**, 159 (2003).
23. A. Beckmann, K.D. Bokle, and D. Elke. Z. Phys. **270**, 173 (1974).
24. E. Arimondo, M. Inguscio, and P. Violino. Rev. Mod. Phys. **49**, 31 (1977).
25. X.X. Guan and Z.W. Wang. Eur. Phys. J. D, **2**, 21 (1998).
26. N. Yamanaka. J. Phys. Soc. Jpn. **68**, 2561 (1999).
27. M. Goedfroid, C.F. Fischer, and P. Jonsson. J. Phys. B, **34**, 1079 (2001).
28. Z.-C. Yan and G.W.F. Drake. Phys. Rev. A, **66**, 042504 (2002).
29. B.A. Bushaw, W. Nörtershäuser, G. Ewald, A. Dax, and G.W.F. Drake. Phys. Rev. Lett. **91**, 043004-1 (2003).
30. K.C. Brog, T.G. Eck, and H. Wider. Phys. Rev. **153**, 91 (1966).
31. H. Orth, H. Ackermann, and E.W. Otten. Z. Phys. A, **23**, 221 (1975).
32. L. Windholz and M. Musso. Z. Phys. D, **8**, 239 (1988).